Scanning tunneling microscopy of the formation, transformation, and property of oligothiophene self-organizations on graphite and gold surfaces

Article *in* Proceedings of the National Academy of Sciences · April 2007

DOI: 10.1073/pnas.0611585104 · Source: PubMed

CITATIONS
55

READS
74

7 authors, including:

Zhi-Yong Yang
Chinese Academy of Sciences
18 PUBLICATIONS **335** CITATIONS

SEE PROFILE

Wei-Guo Song
Chinese Academy of Sciences
135 PUBLICATIONS **11,243** CITATIONS

SEE PROFILE

Scanning tunneling microscopy of the formation, transformation, and property of oligothiophene self-organizations on graphite and gold surfaces

Zhi-Yong Yang*†, Hui-Min Zhang*, Cun-Ji Yan*†, Shan-Shan Li*†, Hui-Juan Yan*, Wei-Guo Song*, and Li-Jun Wan*‡

*Beijing National Laboratory for Molecular Sciences, Institute of Chemistry, and †Graduate School, The Chinese Academy of Sciences, Beijing 100080, People's Republic of China

Communicated by Chunli Bai, The Chinese Academy of Sciences, Beijing, People's Republic of China, December 29, 2006 (received for review October 2, 2006)

Two alkyl-substituted dual oligothiophenes, quarterthiophene (4T)-trimethylene (tm)-octithiophene (8T) and 4T-tm-4T, were used to fabricate molecular structures on highly oriented pyrolytic graphite and Au(111) surfaces. The resulted structures were investigated by scanning tunneling microscopy. The 4T-tm-8T and 4T-tm-4T molecules self-organize into long-range ordered structures with linear and/or quasi-hexagonal patterns on highly oriented pyrolytic graphite at ambient temperature. Thermal annealing induced a phase transformation from quasi-hexagonal to linear in 4T-tm-8T adlayer. The molecules adsorbed on Au(111) surface in randomly folded and linear conformation. Based on scanning tunneling microscopy results, the structural models for different self-organizations were proposed. Scanning tunneling spectroscopy measurement showed the electronic property of individual molecules in the patterns. These results are significant in understanding the chemistry of molecular structure, including its formation, transformation, and electronic properties. They also help to fabricate oligothiophene assemblies with desired structures for future molecular devices.

phase transition | self-assembly | molecular structure

Thiophene derivatives, including oligothiophene (1–5), cyclothiophene (6–8), and polythiophene (9), are currently receiving considerable attention because of their well defined chemical structures, improved solubilities, and various electronic properties (10, 11). They are promising materials in electronic and optical devices such as Schottky diodes (12), organic light-emitting diodes (OLEDs) (13, 14), field-effect transistors (15), and organic thin film transistors (11, 16). For example, the transistors fabricated with thiophene derivatives shows high charge-carrier mobility, high on/off modulation ratio, and long life (15). By modifying molecular structures with functional groups, alkyl chains and thiophene rings, the emitting color of an OLED can be regulated from blue to red (17).

The property of a molecular assembly is governed by not only the property of individual molecules but also the spatial arrangement of the molecules in the assembly (10, 18, 19). Therefore, understanding the molecular arrangement and single molecule's property on substrate surface is very important in fabricating thiophene-based devices. Previous studies have demonstrated that most thiophene molecules can self-organize and form adlayer structures when they adsorb on certain substrates. With fine balance between intermolecular interactions and molecule/substrate interactions, the molecular structures can be varied, resulting in desirable functionalities (20).

The direct observation and investigation of molecular nanostructures at solid surfaces is a constant challenge in molecular science. Scanning probe microscopy, in particular, scanning tunneling microscopy (STM), is the most potent tool for studying the molecules adsorbed onto a solid substrate (20–24). With recent developments in this field, it is now possible to obtain submolecular- or even atomic-resolution images of self-organized molecular structures, identify device-like characteristics in these structures, and create new structures.

Alkyl-substituted oligothiophenes are important thiophene derivatives with novel properties (10, 11). Several STM studies have demonstrated the adsorption possibility of several thiophene derivative molecules on various substrates. Stabel and Rabe (10) reported a STM study of α,ω-dihexylsexithiophene on highly oriented pyrolytic graphite (HOPG) surface. Azumi *et al.* (25) reported several α-alkylated quarterthiophenes (4Ts) adsorbed on a molybdenum disulfide (MoS_2) surface. The arrangement of molecules in the assembly is influenced by introducing a polarizable halogen group to the conjugated backbone (26). Müller *et al.* (27) reported novel substituted dialkylquinquethiophenes on HOPG. They found that the formyl substitutions affect the molecular assemblies. Recently, we (28) reported a STM study of the molecular architectures of alkyl-substituted oligothiophenes on HOPG through hydrogen bonds, in which a series of oligothiophenes with carboxylic groups and different alkyl chains were synthesized and studied. The alkyl chains and carboxylic groups, which were subjected to hydrogen-bond interactions, were purposefully attached to different positions of the oligothiophenes. We found that the hydrogen bond played an essential role in the formation of the ordered assemblies. A controlled 2D molecular assembly was fabricated through hydrogen bonds.

In this article, we describe the self-organizations of two alkyl-substituted dual oligothiophenes. The molecules are unsymmetrical 4T-trimethylene (tm)-octithiophene (8T) and symmetrical 4T-tm-4T, where one 4T and one 8T or two 4Ts are linked by a tm. Two hexyl groups are attached to each 4T, and four hexyl groups are attached to each 8T. The chemical structures of the two molecules are shown in Scheme 1. These molecules have well defined chemical structures and may bring promising properties for electronic and optical device (29, 30). The molecules are deposited onto HOPG and Au(111) surfaces and are investigated by STM. Scanning tunneling spectroscopy (STS) with STM tip to collect local I–V characteristics is used to measure the electronic property of the self-organized structures. Both molecules form adlayers on HOPG and Au(111). The ordering of the adlayers depends on the substrates. Linear and quasi-hexagonal structures of 4T-tm-8T molecules are seen on HOPG surface at ambient temperature. After thermal anneal-

Author contributions: L.-J.W. designed research; Z.-Y.Y., H.-M.Z., C.-J.Y., S.-S.L., and H.-J.Y. performed research; Z.-Y.Y., C.-J.Y., S.-S.L., H.-J.Y., and L.-J.W. analyzed data; Z.-Y.Y., W.-G.S., and L.-J.W. wrote the paper; and L.-J.W. supervised the research work.

The authors declare no conflict of interest.

Abbreviations: HOPG, highly oriented pyrolytic graphite; STM, scanning tunneling microscopy; STS, scanning tunneling spectroscopy; 4T, quarterthiophene; 8T, octithiophene; tm, trimethylene; LUMO, lowest unoccupied molecular orbital; HOMO, highest occupied molecular orbital.

‡To whom correspondence should be addressed. E-mail: wanlijun@iccas.ac.cn.

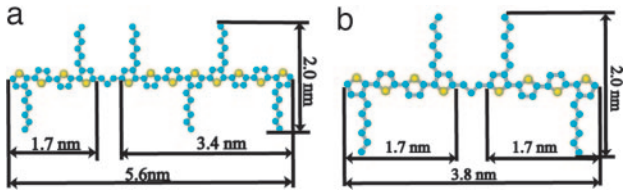

Scheme 1. Chemical structure of 4T-tm-8T (*a*) and 4T-tm-4T (*b*).

ing, a structural transformation is observed in 4T-tm-8T adlayer. These results are significant in fabricating oligothiophene molecular assembly and understanding the mechanism of structural formation and transformation of the assembly, which is of prime importance in future development of functional nanostructures and devices.

Results and Discussion

Self-Organization of 4T-tm-8T. ***Quasi-hexagonal structure on HOPG.*** STM observation shows that 4T-tm-8T form both quasi-hexagonal and linear adlayers. Fig. 1*a* is a large-scale STM image acquired in the quasi-hexagonal domain. The 4T-tm-8T molecules form a well defined adlayer extending to >100 nm on HOPG surface. The distinct feature in the image is the bright elliptical rings with dark depressions in the center, forming an adlayer structure in quasi-hexagonal symmetry.

To reveal the structural details of the quasi-hexagonal adlayer, high-resolution STM images are acquired. Fig. 1*b* is a typical high-resolution STM image expanded from Fig. 1*a*. The adlayer is extended in direction **A** and **B**. The distance between neighboring dark depressions along direction **A** is a = 4.3 ± 0.2 nm, and along direction **B** is b = 3.5 ± 0.2 nm. The angle between direction **A** and **B** is α = 58 ± 2°. A unit cell for the adlayer is outlined in Fig. 1*b*. The distance between two bright strands in two neighbor elliptical unit is d = 1.3 ± 0.2 nm, consistent with a previous report on oligo(hexylthiophene)s (31).

Close examination of the STM images shows that each elliptical ring has two long parts and two short parts. The length of the short part is L1 = 1.7 ± 0.2 nm and the long part is L2 = 3.3 ± 0.2 nm, which agrees very well with the lengths of 4T and 8T in a 4T-tm-8T molecule, respectively. Based on these findings we propose that each elliptical ring is composed of two 4T-tm-8T molecules, which bend and pair with each other to form the special ring morphology as schematically illustrated in Fig. 1*b*. During the STM experiments, we occasionally observed STM images (Fig. 1*b Inset*). There are half-elliptical rings indicated by two arrows in Fig. 1*b*. Each half-elliptical ring corresponds to an unpaired 4T-tm-8T molecule, which bends and looks like half of the elliptical ring. The presence of such half-elliptical rings is a direct evidence for our notion that each elliptical ring is composed of two 4T-tm-8T molecules.

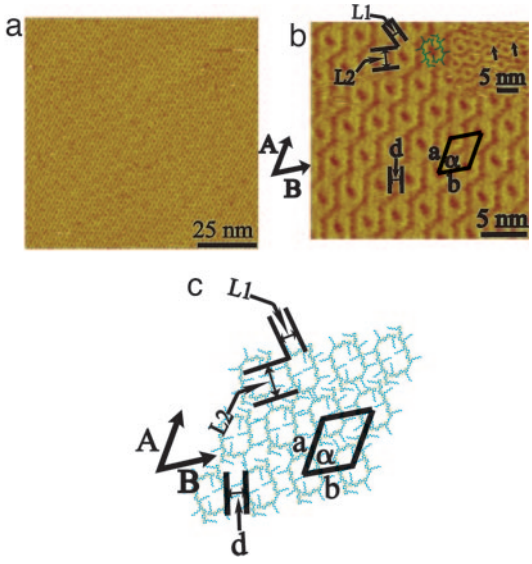

Fig. 1. STM images and model of 47-tm-8T quasi-hexagonal adlayer. (*a*) Large-scale STM image of 4T-tm-8T adlayer on HOPG in a quasi-hexagonal symmetry. The tunneling current is 0.724 nA with a bias of 0.6 V. (*b*) High-resolution STM image of *a*. The tunneling current is 0.651 nA with a bias of −0.6 V. (*Inset*) The tunneling current is 0.611 nA with a bias of 0.698 V. (*c*) Structural model of the 4T-tm-8T quasi-hexagonal adlayer.

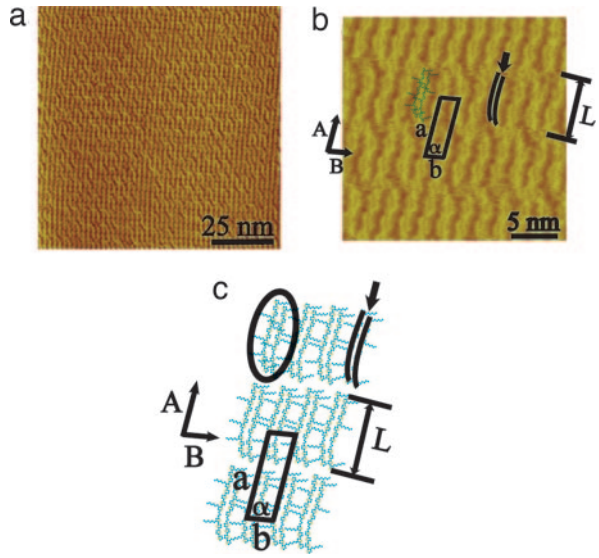

Fig. 2. STM images and model of 47-tm-8T linear adlayer. (*a*) Large-scale STM image of 4T-tm-8T linear adlayer on HOPG. The tunneling current is 0.644 nA with a bias of −0.508 V. (*b*) High-resolution STM image of *a*. The imaging conditions are the same as those in *a*. (*c*) Proposed structural model of the linear adlayer.

A structural model for the quasi-hexagonal adlayer is shown in Fig. 1*c*. Two 4T-tm-8T molecules fold into a "bracket," which appears in the bright elliptical ring with a depression. The short and long parts in each elliptical ring correspond to the 4T and 8T parts of a 4T-tm-8T molecule. In this model, the molecules take an *anti* conformation to reduce the steric hindrance, which implies that all alkyl chains align alternatively along opposite sides of the conjugated oligothiophene backbones.

Linear structure on HOPG. Fig. 2*a* is a large-scale STM image showing linear molecular rows. Fig. 2*b* is a high-resolution STM image from the linear adlayer. The adlayer is composed of short strands. The length of each strand is L = 5.6 ± 0.2 nm, close to the length of a 4T-tm-8T molecule along its thiophene backbone. Because of the flexibility of the oligothiophene molecule, the strands are in a twisted configuration rather than a straight line. Careful observation found that each strand is composed of two substrands (marked by two black lines in Fig. 2*b*). The space between the two substrands is indicated by an arrow in Fig. 2*b*. Each substrand corresponds to a 4T-tm-8T molecule. In the linear adlayer, the molecular rows are extending in **A** and **B** directions. The angle between **A** and **B** directions is α = 79 ± 2°. In direction **A**, the molecules link with each other and form molecular lines with a repeating period of a = 5.9 ± 0.2 nm; whereas in direction **B**, the intermolecular distance is b = 2.1 ± 0.2 nm. A unit cell for the adlayer is deduced from the STM images. The molecular model and unit cell are illustrated in Fig. 2*b*.

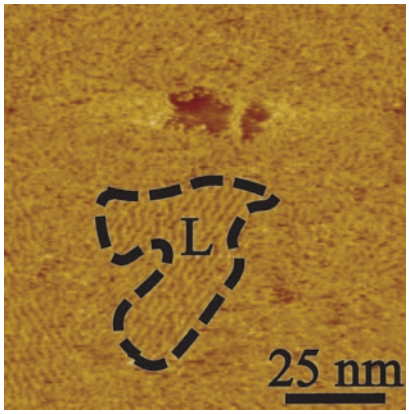

Fig. 3. STM image after annealing 4T-tm-8T adlayer at 100°C in ambient condition. The tunneling current is 0.648 nA with a bias of 0.62 V.

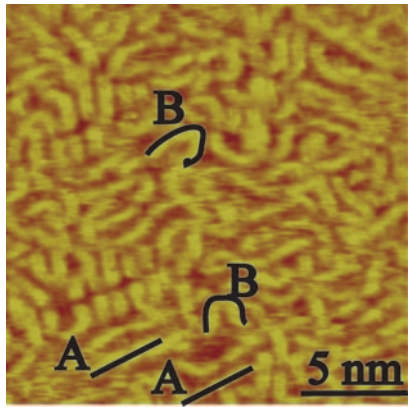

Fig. 4. STM image of 4T-tm-8T adlayer on Au(111) in 0.1 M $HClO_4$ at 0.532 V. The tunneling current is 0.827 nA with a bias of −0.186 V.

By theoretical calculation, STM imaging, and x-ray analysis of 3D bulk oligothiophene materials, Mena-Osteritz (32) identified various possible conformations of oligothiophenes on HOPG surface. Extended arrays and chain foldings were found. For example, poly(3-dodecylthiophene) formed straight and folded structure with both *anti* and *syn* conformation, which demonstrated the flexibility and conformational diversity of the oligothiophenes. In this study, the arrangement of the oligothiophene moieties is expected to be in *anti* conformation from STM image features and the previous theoretical calculation. All alkyl chains would be perpendicular to their conjugated backbones and interdigitate alkyl chains on the neighboring strands. However, the possibility that some alkyl chains may extend out of the HOPG surface cannot be excluded. Such a conformation may also reduce the steric hindrance in adlayer. Further study to determine the exact conformation of the alkyl chains is required.

A structural model for the linear adlayer is illustrated in Fig. 2*c*. In this model, two 4T-tm-8T molecules pair with each other in a strand. For clearer illustration, only one pair of molecules surrounded by an ellipse is drawn with all alkyl chains. Other 4T-tm-8T molecular models in Fig. 2 *b* and *c* are shown with only half of the side alkyl chains; a pair of black lines is used to represent a strand consisting of two molecules, and an arrow indicates the space between two molecules.

Structural transformation. On the HOPG surface, two adlayer domains with linear or quasi-hexagonal structures can be observed simultaneously as shown in Figs. 1 and 2, which indicate two relatively stable conformations of the self-organized structures. It is well known that self-organized structures will transform into a more stable structure with increasing temperature. For a molecular device, understanding the structural transformation and temperature effect on the adlayer structure is very important in terms of device stability and efficiency (33, 34). After investigating the adlayer structures in the quasi-hexagonal and linear regions, we annealed the sample to investigate the structural transformation. Fig. 3 is a typical STM image after the sample was annealed at 100°C for 30 min. Fig. 3 shows that only linear domain can still be seen after annealing, and the domain size is substantially decreased. Quasi-hexagonal domains completely disappear. Another feature in the STM image is the disordered domain, which dominates the image. The results demonstrate a structural transformation from quasi-hexagonal to linear arrangement and finally disordered structure after annealing. In the linear assembly, the conjugated oligothiophene backbones will be extended upon heating, which would decrease the steric hindrance and result in a more stable adlayer.

Self-organization of 4T-tm-8T on Au(111). Substrates can influence the adlayer structures by different molecule/substrate interactions (21). For a comparison, we prepared an assembly with 4T-tm-8T molecules on Au(111) surface. Fig. 4 shows a typical STM image of the adlayer. The molecules adsorb on Au(111) surface without long-range ordering, showing the substrate effect on adlayer structures.

In Fig. 4 the molecules appear in bright strands with linear and bent conformation in their conjugated oligothiophene backbones. In Fig. 4 two straight lines marked **A** indicate two linear strands, and two U-shape strands marked **B** indicate bent molecules. In a linear conformation, the 4T-tm-8T molecule is expected to adsorb on Au(111) with its thiophene rings parallel to the surface, taking the most energetically favorable geometry. When 4T-tm-8T molecules bend on the surface, some thiophene rings are forced to rotate. The same hairpin folding of molecular backbone is also reported in a study of poly(3-hexylthiophene) and poly(3-dodecylthiophene) adlayers on the HOPG surface (31, 32). The energy necessary to rotate one of the thiophenes from an *anti* into a *syn* conformation is, depending on the substituent on the β-position, ≈12–20 kJ/mol (31). Therefore, the 4T-tm-8T molecules can take both linear and folded arrangement on the Au(111) surface.

Self-Organization of 4T-tm-4T. ***4T-tm-4T on HOPG.*** Compared with 4T-tm-8T molecules, 4T-tm-4T molecules show higher symmetry in its chemical structure. To understand the effect of molecular structure on the self-organized molecular structures, we prepared 4T-tm-4T adlayer on HOPG.

Fig. 5*a* is a typical large-scale STM image recorded on a 4T-tm-4T adlayer on HOPG. The molecules self-organize into long-range ordering with regular molecular rows. The molecular rows extend along directions **A** and **B**. The angle between **A** and **B** is 84 ± 2°. In direction **A**, the molecular rows appear in wave-like configuration.

Fig. 5*b* is a high-resolution STM image of the 4T-tm-4T adlayer, indicating that each strand consists of a pair of substrands. The space between the two substrands is indicated by an arrow. The distance between the centers of two substrands in a pair is d1 = 0.6 ± 0.2 nm. Careful observation reveals that each substrand corresponds to a 4T-tm-4T molecule. Because of the molecular flexibility, the molecules adsorb on the HOPG surface in a sinuous line, resulting in a wave-like appearance. L1 and L2 have equal lengths of 1.7 ± 0.2 nm, consistent with the length of the 4T part in 4T-tm-4T. The distance between neighboring strands is d2 = 2.0 ± 0.2 nm. A unit cell for the adlayer is outlined in Fig. 5*b* with a = 4.1 ± 0.2 nm, b = 4.0 ± 0.2 nm, and α = 84 ± 2°.

A structural model for the molecular adlayer is proposed in Fig. 5*c*. Two 4T-tm-4T molecules form a strand. Note in the

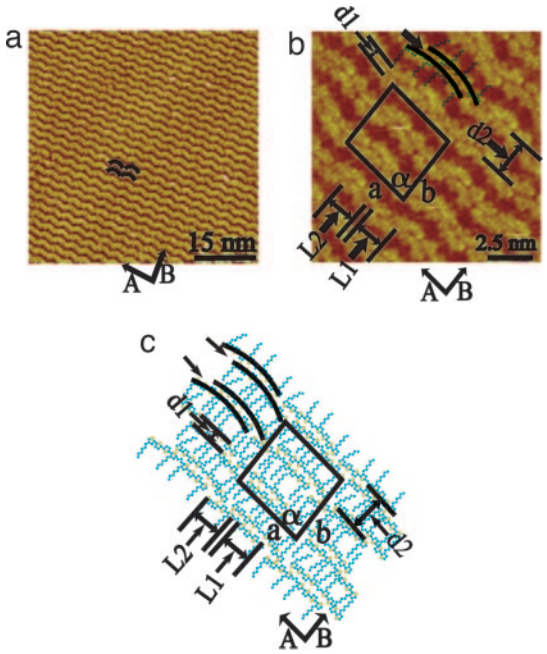

Fig. 5. STM images and model of 4T-tm-4T adlayer. (*a*) Large-scale STM image of 4T-tm-4T adlayer on HOPG. The tunneling current is 0.767 nA with a bias of 0.650 V. (*b*) High-resolution STM image of *a*. The tunneling current is 0.642 nA with a bias of 0.395 V. (*c*) Structural model of the 4T-tm-4T adlayer.

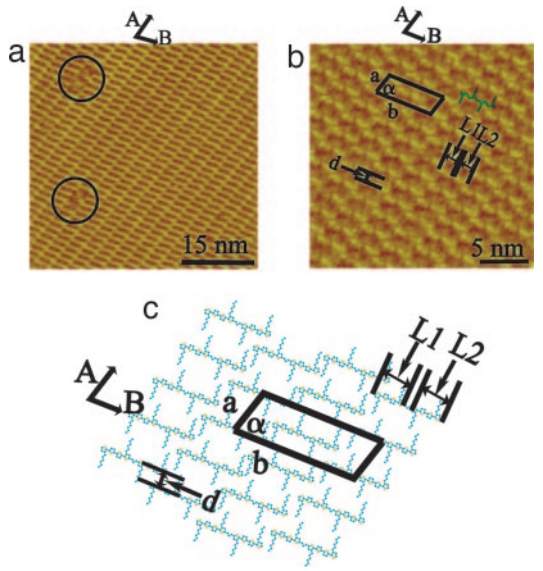

Fig. 6. STM images and model of 4T-tm-4T adlayer. (*a*) Large-scale STM image of 4T-tm-4T adlayer on HOPG. The tunneling current is 0.685 nA with a bias of −0.763 V. (*b*) High-resolution STM image of *a*. The tunneling current is 0.61 nA with a bias of −0.763 V. (*c*) Structural model for the 4T-tm-4T adlayer.

model that the molecules are proposed to be in a *syn* conformation. In the *syn* conformation, alkyl chains between neighboring molecules interdigitate each other, resulting in a stable adlayer. The other structural feature in the model is the position displacement of two molecules in a strand as shown in Fig. 5*c*, which depicts the molecular models of the structure. With the position displacement the alkyl chains in neighboring strands can well interdigitate and decrease the steric hindrance.

Although most of the adlayer appears in the structure as Fig. 5*a* shows, very occasionally, we observed another molecular domain as shown in Fig. 6. Fig. 6*a* is a large-scale STM image of the domain. Although several molecular defects (circled in Fig. 6*a*) can be seen in this image, molecules form a well defined adlayer. The adlayer appears in a lamella structure extending in directions **A** and **B**.

More structural information is obtained in a high-resolution STM image in Fig. 6*b*. The adlayer is composed of straight short "sticks" with a small black gap in the center of each stick. The gap divides a stick into two parts. The size of these two parts is measured to be L1 = 1.7 ± 0.2 nm and L2 = 1.7 ± 0.2 nm, close to the size of the 4T. The length of a stick is 3.8 ± 0.2 nm, consistent with the size of a 4T-tm-4T. Therefore, each stick represents a 4T-tm-4T molecule. The center black gap in a molecule is attributed to the tm, which has low electron density. A molecular model is illustrated in Fig. 6*b*. The intermolecular distance along direction **A** is a = 2.9 ± 0.2 nm, and along direction **B** is b = 6.0 ± 0.2 nm. The angle between **A** and **B** directions is $\alpha = 73 \pm 2°$. From the molecular arrangement, a unit cell is deduced and outlined in Fig. 6*b* with a = 2.9 ± 0.2 nm, b = 6.0 ± 0.2 nm, and $\alpha = 73 \pm 2°$. It is interesting that there is a displacement in the neighboring molecular rows along direction **B**. The displacement is d = 1.2 ± 0.2 nm.

A structural model for the 4T-tm-4T adlayer is proposed in Fig. 6*c*. The molecules adsorb on the HOPG surface in a parallel orientation, and all alkyl chains align alternatively along the opposite side of the conjugated oligothiophene backbones. The alkyl chains at two ends of molecules interdigitate and cause a displacement of 1.2 nm, consistent with the measurement in Fig. 6*b*. On the other hand, the results in Fig. 6 show the difference in appearance of a 4T-tm-4T molecule on the HOPG surface in its *syn* and *anti* conformations. In an *anti* conformation, the molecule appears in a straight short stick, whereas a distorted strand is formed from *syn* conformation.

4T-tm-4T on Au(111). The adsorption of 4T-tm-4T molecules is also investigated on an Au(111) surface. Fig. 7 is an STM image of the adlayer of 4T-tm-4T on Au(111). Similar to 4T-tm-8T, a random adsorption is observed in the image. Linear and folded conformation of the molecules can be seen, as indicated by **A** and **B,** respectively. The results once again demonstrate the effect of the substrate on the molecular adlayer formation (21, 35). Understanding the intermolecular interaction and molecule/substrate is very important in fabricating devices by alkyl-substituted oligothiophene molecules. The interaction between molecule and substrate on HOPG is usually weaker than that on an Au surface. On a HOPG surface, the molecules have higher mobility and can easily self-organize into ordered structure. However, on an Au(111) surface, the stronger molecule/

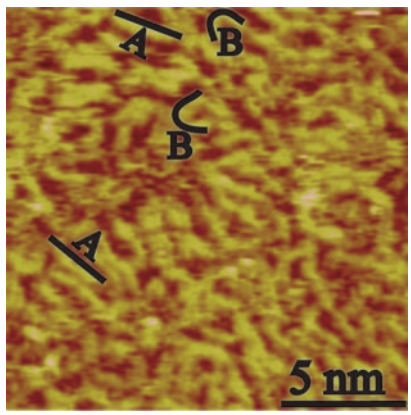

Fig. 7. STM image of 4T-tm-4T adlayer on Au(111) in 0.1 M $HClO_4$ at 0.520 V. The tunneling current is 0.742 nA with a bias of −0.174 V.

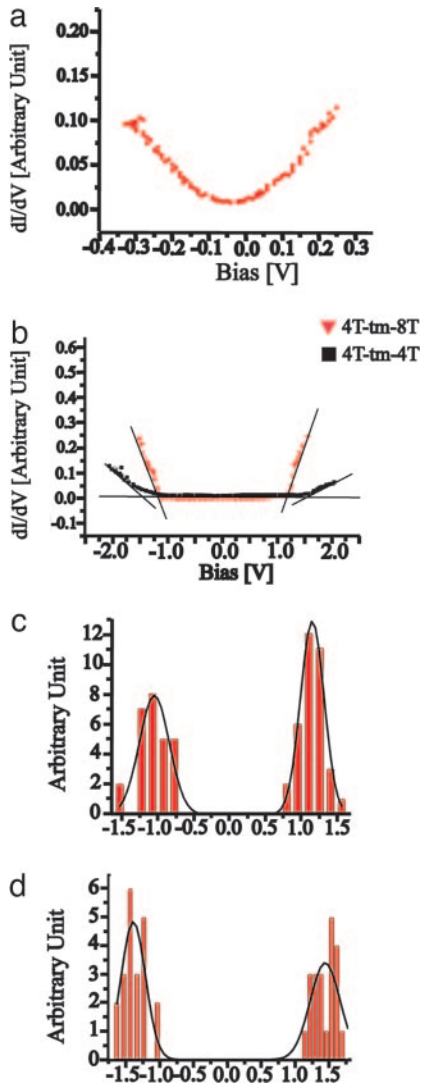

Fig. 8. STS results of bare HOPG, 4T-tm-8T, and 4T-tm-4T. (*a*) Typical *dI/dV-V* curve obtained on bare HOPG. (*b*) Typical *dI/dV-V* curve obtained on 4T-tm-8T and 4T-tm-4T adlayers on HOPG in ambient condition. (*c*) The histogram of experimental gap edges of 4T-tm-8T molecules. The black solid lines show a G fit of the columns. (*d*) The histogram of experimental gap edges of 4T-tm-4T molecules. The black solid lines show a G fit of the columns.

substrate interaction will decrease the mobility of the adsorbate and cause a random adsorption.

STS Results and Discussion. To probe the electronic properties of 4T-tm-8T and 4T-tm-4T molecules on HOPG under ambient condition, we performed STS measurements of the adlayers. For comparison, *dI/dV-V* curve on bare graphite was also measured. As shown in Fig. 8*a*, the curve has a characteristic parabola shape, and no apparent energy gap is found because of high conductivity of the graphite.

Fig. 8*b* shows the typical *dI/dV-V* curves from the adlayers of 4T-tm-8T and 4T-tm-4T. The *dI/dV-V* curve reflects the density states of adsorbates. When applying an appropriate bias on substrate, the Fermi energy of the substrate will resonate with certain molecular orbits of adsorbate molecules, either highest occupied molecular orbital (HOMO) or lowest unoccupied molecular orbital (LUMO), and induce sharp change in the *dI/dV-V* curve. The edge defined by the cross-point of the tangents of the platform and uplift part of the curve represents the energy states of HOMO and LUMO of the adsorbate molecules (34). Thus experimentally the energy gap between HOMO and LUMO is measured as the separation between these two edges.

The histograms in Fig. 8 *c* and *d* show the statistic distributions of the edges of HOMO and LUMO measured from a large number of spectra from 4T-tm-8T and 4T-tm-4T adlayers. The experimental energy gap is given by Gaussian simulation. The statistic results reveal that the left and right edge for 4T-tm-8T are at -1.05 ± 0.2 eV and 1.12 ± 0.2 eV, respectively, and for 4T-tm-4T the left and right edge are at -1.40 ± 0.2 eV and 1.44 ± 0.2 eV, respectively. The results show that the centers of energy gaps in both 4T-tm-8T and 4T-tm-4T are slightly shifted to positive regions, consistent with the previous report that oligothiophene is a *p*-type material in air (7). The experimental energy gap is 2.17 ± 0.4 eV for 4T-tm-8T and 2.84 ± 0.4 eV for 4T-tm-4T. Theoretical simulation (Material Studio 3.1; density functional theory) shows that both HOMO and LUMO of 4T-tm-8T are located mainly on the 8T part; whereas for 4T-tm-4T, the HOMO is located on one 4T part and the LUMO is located on the other 4T part. For comparison, previous research (36) found that the energy gap for 8T and 4T is ≈2.41 eV and 3.13 eV, respectively. STM results in the present study indicate that alkyl-substituted oligothiophenes molecules still preserve their electronic properties in the ordered molecular adlayer on the HOPG surface. This result is very significant in designing molecular devices.

In summary, the self-assemblies and properties of two dual oligothiophenes, 4T-tm-8T and 4T-tm-4T, were investigated on HOPG and Au(111) surfaces by STM and STS. On HOPG, both 4T-tm-8T and 4T-tm-4T form highly ordered adlayers. For 4T-tm-8T, linear and quasi-hexagonal adlayers are observed. After annealing, only linear adlayer is seen. For 4T-tm-4T, wave-like adlayer dominates, and the lamella structure of 4T-tm-4T is very occasionally observed. In contrast, random adsorption of the two molecules is seen on the Au(111) surface, demonstrating the substrate effect on the self-organization of molecules. STS experiment reveals characteristics of *p*-type semiconductor for 4T-tm-8T and 4T-tm-4T adlayers, with energy gaps of 2.2 eV and 2.8 eV, respectively. These results can help fabricate oligothiophene assembly through a bottom-up strategy and are important in understanding the effect of molecule/molecule and molecule/substrate interactions on the self-organized molecular structure's formation and transformation.

Materials and Methods

Chemicals. 4T-tm-8T and 4T-tm-4T were prepared as described (29). Toluene (analytic grade) was from the Beijing Shunyi Chemical Factory (Beijing, People's Republic of China).

Substrates. HOPG (quality ZYB) was from Digital Instruments (Santa Barbara, CA). Au singe-crystal beads with (111) faces exposed were prepared by melting an Au wire (99.999%) (37, 38). These two substrates were used for molecule assembling and STM experiments. Before molecular adlayer formation, the Au(111) surface was quenched in a hydrogen-saturated ultrapure water (Milli-Q; ≥18.2 MΩ; Millipore, Billerica, MA) to obtain a clean substrate surface.

Molecular Adlayers and STM Measurements. On HOPG surface, the adlayer was prepared by depositing a drop (≈2 μl) of toluene solution containing $\approx 10^{-5}$ M 4T-tm-8T or 4T-tm-4T onto freshly cleaved HOPG with an atomically flat surface (35). After evaporation of the solvent, the STM experiments were carried out in atmosphere with a Nanoscope IIIa scanning probe microscope (Digital Instruments). STM tips were made from mechanically cut Pt/Ir wire (90/10). On the Au(111) surface, the molecular adlayers were prepared by immersing the single-

crystal Au bead into the above-mentioned solution containing the sample molecules for 3–5 min (35, 39). After formation of the molecular adlayer, the Au bead was thoroughly rinsed with Milli-Q water to remove the remnant molecules and mounted into the STM electrochemical cell. The STM experiments were carried out with a Nanoscope E scanning tunneling microscope (Digital Instruments) in $HClO_4$ solution prepared by diluting ultrapure $HClO_4$ (Cica-Merck, Kanto Kagaku, Japan) with Milli-Q water, under potential control at double layer potential region. The typical potentials used in this experiment were between 510 and 550 mV. All potentials are reported with respect to the reversible hydrogen electrode in 0.1 M $HClO_4$. The tunneling tips were prepared by electrochemically etching a tungsten wire (0.25 mm in diameter) in 0.6 M KOH and an ac voltage of 12–15 V. Then the tungsten tips were coated with a clear nail polish to minimize the faradic current. All of the STM images were obtained in the constant-current mode and without further processing such as high pass or filtering treatment. The tunneling conditions used in the experiments are given in the figure legends.

STS experiments were performed by applying a modulation (peak-to-peak 0.02 V to 0.03 V) to the bias voltage. A lock-in amplifier was used to collect the *dI/dV-V* signals. The feedback of the STM control was turned off during STS measurements.

We thank Drs. Yasuyuki Araki and Osamu Ito (Institute of Multidisciplinary Research for Advanced Materials, Tohoku University, Sendai, Japan) and Kazuo Takimiya and Tetsuo Otsubo (Hiroshima University, Higashi-Hiroshima City, Japan) for providing samples. This work is supported by National Natural Science Foundation of China Grants 20520140277, 20575070, 20673121, 20673125, and 20121301; National Key Project on Basic Research Grants 2006CB806100 and 2006CB932100; and the Chinese Academy of Sciences.

1. Azumi R, Götz G, Debaerdemaeker T, Bäuerle P (2000) *Chem Eur J* 6:735–744.
2. Bäuerle P (1992) *Adv Mater* 4:102–107.
3. Bäuerle P, Fischer T, Bidlingmeier B, Stabel A, Rabe JP (1995) *Angew Chem Int Ed* 34:303–307.
4. Leclère P, Surin M, Viville P, Lazzaroni R, Kilbinger AFM, Henze O, Feast WJ, Cavallini M, Biscarini F, Schenning APHJ, Meijer EW (2004) *Chem Mater* 16:4452–4466.
5. Gong JR, Yan HJ, Yuan QH, Xu LP, Bo ZS, Wan LJ (2006) *J Am Chem Soc* 128:12384–12385.
6. Krömer J, Rios-Carreras I, Fuhrmann G, Musch C, Wunderlin M, Debaerdemaeker T, Mena-Osteritz E, Bäuerle P (2000) *Angew Chem Int Ed* 39:3481–3486.
7. Mena-Osteritz E, Bäuerle P (2006) *Adv Mater* 18:447–451.
8. Mena-Osteritz E, Bäuerle P (2001) *Adv Mater* 13:243–246.
9. Wakabayashi R, Kubo Y, Kaneko K, Takeuchi M, Shinkai S (2006) *J Am Chem Soc* 128:8744–8745.
10. Stabel A, Rabe JP (1994) *Synth Met* 67:47–53.
11. Murphy AR, Fréchet JMJ, Chang P, Lee J, Subramanian V (2004) *J Am Chem Soc* 126:1596–1597.
12. Yassar A, Demanze F, Fichou D (1999) *Opt Mater* 12:379–382.
13. Mazzeo M, Pisignano D, Favaretto L, Barbarella G, Cingolani R, Gigli G (2003) *Synth Met* 139:671–673.
14. Friend RH, Gymer RW, Holmes AB, Burroughes JH, Marks RN, Taliani C, Bradley DDC, Dos Santos DA, Brédas JL, Lögdlund M, Salaneck WR (1999) *Nature* 397:121–128.
15. Huisman B-H, Valeton JJP, Nijssen W, Lub J, ten Hoeve W (2002) *Adv Mater* 15:2002–2005.
16. Videlot-Ackermann C, Ackermann J, Brisset H, Kawamura K, Yoshimoto N, Raynal P, El Kassmi A, Fages F (2005) *J Am Chem Soc* 127:16346–16347.
17. Li ZH, Wong MS, Fukutani H, Tao Y (2005) *Chem Mater* 17:5032–5040.
18. Metzger RM (1999) *Acc Chem Res* 32:950–957.
19. Prato S, Floreano L, Cvetko D, De Renzi V, Morgante A, Modesti S, Biscarini F, Zamboni R, Taliani C (1999) *J Phys Chem B* 103:7788–7795.
20. Hermann BA, Scherer LJ, Housecroft CE, Constable EC (2006) *Adv Funct Mater* 16:221–235.
21. Wan LJ (2006) *Acc Chem Res* 39:334–342.
22. Hamers RJ (1996) *J Phys Chem* 100:13103–13120.
23. Noda H, Wan LJ, Osawa M (2001) *Phys Chem Chem Phys* 3:3336–3342.
24. Gesquière A, De Feyter S, De Schryver FC, Schoonbeek F, van Esch J, Kellogg RM, Feringa BL (2001) *Nano Lett* 1:201–206.
25. Azumi R, Götz G, Bäuerle P (1999) *Synth Met* 101:569–572.
26. Abdel-Mottaleb MMS, Götz G, Kilickiran P, Bäuerle P, Mena-Osteritz E (2006) *Langmuir* 22:1443–1448.
27. Müller H, Petersen J, Strohmaier R, Gompf B, Eisenmenger W, Vollmer MS, Effenberger F (1996) *Adv Mater* 8:733–737.
28. Xu LP, Gong JR, Wan LJ, Jiu TG, Li YL, Zhu DB, Deng K (2006) *J Phys Chem B* 110:17043–17049.
29. Narutaki M, Takimiya K, Otsubo T, Harima Y, Zhang H, Araki Y, Ito O (2006) *J Org Chem* 71:1761–1768.
30. Sakai T, Satou T, Kaikawa T, Takimiya K, Otsubo T, Aso Y (2005) *J Am Chem Soc* 127:8082–8089.
31. Mena-Osteritz E, Meyer A, Langeveld-Voss BMW, Janssen RAJ, Meijer EW, Bäuerle P (2000) *Angew Chem Int Ed* 39:2680–2684.
32. Mena-Osteritz E (2002) *Adv Mater* 14:609–616.
33. Rohde D, Yan CJ, Yan HJ, Wan LJ (2006) *Angew Chem Int Ed* 45:3996–4000.
34. Gong JR, Wan LJ, Lei SB, Bai CL, Zhang XH, Lee S-T (2005) *J Phys Chem B* 109:1675–1682.
35. Gong JR, Wan LJ, Yuan QH, Bai CL, Jude H, Stang PJ (2005) *Proc Natl Acad Sci USA* 102:971–974.
36. Bouzzine SM, Bouzakraoui S, Bouachrine M, Hamidi M (2005) *J Mol Struct (Theochem)* 726:271–276.
37. Wan LJ, Shundo S, Inukai J, Itaya K (2000) *Langmuir* 16:2164–2168.
38. Wan LJ, Terashima M, Noda H, Osawa M (2000) *J Phys Chem B* 104:3563–3569.
39. Yoshimoto S, Higa N, Itaya K (2004) *J Am Chem Soc* 126:8540–8545.